

# Effects of Activation Temperature on the Properties and Structure of PAN-Based Activated Carbon Hollow Fiber

Junfen Sun, Qingrui Wang

State Key Laboratory for Modification of Chemical Fibers and Polymer Materials, College of Material Science & Engineering, Donghua University, Shanghai 200051, People's Republic of China

Received 2 February 2005; accepted 15 August 2005

DOI 10.1002/app.23519

Published online in Wiley InterScience (www.interscience.wiley.com).

**ABSTRACT:** Polyacrylonitrile (PAN) hollow fibers were pretreated with ammonium dibasic phosphate, then further oxidized in air, carbonized in nitrogen, and activated with carbon dioxide. The effects of activation temperature of a precursor fiber on the microstructure, specific surface, pore-size distribution, and adsorption properties of PAN-based activated carbon hollow fibers (PAN-ACHF) were studied in this work. After the activation process, the BET surface area of the PAN-ACHF and surface area of mesopores in the PAN-ACHF increased very remarkably and reached  $1422 \text{ m}^2 \text{ g}^{-1}$  and  $1234 \text{ m}^2 \text{ g}^{-1}$ , respectively, when activation temperature is  $1000^\circ\text{C}$ . The adsorptions to creatinine and  $\text{VB}_{12}$  of PAN-ACHF were much high and reached 99 and 84% respectively. In PAN-ACHF which went through the activa-

tion at  $700^\circ\text{C}$  and  $800^\circ\text{C}$ , the micropore filling mainly occurred at low relative pressures, multimolecular layer adsorption occurred with the increasing of relative pressure, and the filling and emptying of the mesopores by capillary condensation occurred at high relative pressures. But in PAN-ACHF which went through the activation at  $900^\circ\text{C}$ , a mass of mesopores resulted in the large pore filling by capillary condensation. The dominant pore sizes of mesopores in PAN-ACHF are from 2 nm to 5 nm. © 2006 Wiley Periodicals, Inc. *J Appl Polym Sci* 100: 3778–3783, 2006

**Key words:** activation temperature; polyacrylonitrile; activated carbon hollow fiber; adsorption properties

## INTRODUCTION

Activated carbon has porous structure and is carbonized and activated from carbonic substances such as sawdust, charcoal, coconut shell, various kind of nutshells, as well as macromolecular carbon through the process of physical or chemical activation. It contains a small quantity of hydrogen, oxygen, and some other elements.<sup>1</sup> It has high porosity and, hence, a very large surface area.<sup>2,3</sup> Therefore, all sorts of activated carbon, whatever shapes might be, have adsorbing ability and are widely used in areas including food, pharmaceutical, chemical, national defense, agriculture, water processing, and environment protecting industries.<sup>4</sup> At the beginning of 19th century, researches have been focused on the study of the third generation high performance activated carbon fiber (ACF).<sup>5,6</sup> Activated carbon fiber has the advantage of uniform pore size and makes it possible to control the distribution of the porosity during production upon customer's request. In addition, ACF has the advantages of quick adsorption and desorption, light weight, and convenience for application. ACF has played a major role in adsorption technology over the last few years. Re-

cently, the polyacrylonitrile-based activated carbon hollow fiber (PAN-ACHF) has brought on many investigators' interests,<sup>7–12</sup> since PAN-ACHF shows the largest adsorption capacity among the carbon surfaces.

Ming-Chien Yang and Da-Guang Yu<sup>7–10</sup> studied the structure and properties, pore-size distribution, surface area, and mechanical properties of PAN-ACHF. Linkov et al.<sup>13</sup> reported that hollow fibers have been used for gas separation and show high fluxes and good selectivities. Schindler and Maier<sup>14</sup> obtained a patent for making hollow carbon fiber membrane in which the PAN hollow fiber was pretreated with hydrazine and followed by oxidation and carbonization, and was suitable for separating particles.

In this research, the PAN hollow fibers were dipped in ammonium dibasic phosphate aqueous solution, oxidized in air, carbonized in nitrogen, and activated with carbon dioxide. This study examined the effects of activation temperature of stabilized PAN hollow fiber precursor on the adsorption and structural properties, such as specific surface area, pore size distribution and morphology of PAN-ACHF. We discuss the adsorption properties of the resultant PAN-ACHF to creatinine and  $\text{VB}_{12}$ . According to their molecule sizes, creatinine  $< \text{VB}_{12}$ , the molecule size of creatinine is less than 2 nm and primarily adsorbed by micropores ( $< 2$  nm). However, the molecule size of  $\text{VB}_{12}$  is larger than

Correspondence to: J. Sun (junfensun@sohu.com).

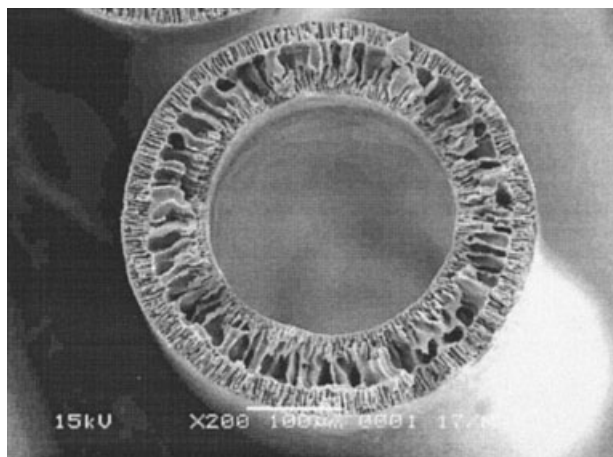


**Figure 1** The cross section of virgin PAN hollow fiber ( $\times 200$ ).

2 nm and primarily adsorbed by mesopores (2–50 nm). There are various types of pores in the ACHF. Macropores have small specific surface area and are thus insignificant to adsorption. However, these pores control the access of adsorbate and also serve as the space for deposition. Mesopores provide channels for the adsorbate to the micropores from the macropores and simultaneously adsorb matter of mesomolecules. As reported in the literature, mesopore can function a capillary condensation, thus it is indispensable for the adsorption of liquid and gas. Micropores determine the adsorption capacity of the ACHF and primarily adsorb the matter of micromolecules. It is the purpose of this paper to discuss what activation process condition provides high surface area and high adsorption ratio for the PAN-ACHF prepared from PAN hollow fibers.

## EXPERIMENTAL

PAN (polyacrylonitrile, a copolymer of acrylonitrile, methyl methacrylate, itaconic acid) hollow fiber spun by dry-wet spinning set up was used as the precursor. The resultant hollow fiber had an inner diameter of 400  $\mu\text{m}$  and an outer diameter of 500  $\mu\text{m}$ . Figure 1 shows the porous structure of the PAN hollow fiber.

Virgin PAN hollow fiber was first dipped in ammonium dibasic phosphate aqueous solution of 4% (wt %) concentration for 30 min. Afterwards, the pre-treated fiber was oxidized in the air at 230°C for 5 h, carbonized in nitrogen at 900°C for 70 min, and activated with carbon dioxide at different temperatures for 40 min.

A scanning electron microscope (SEM) (JEOL Model JSM-5600LV) was used to examine the cross section and external surface of fibers.

Adsorption study to creatinine and  $\text{VB}_{12}$  was carried out by a static process. A known quantity of the

PAN-based activated carbon hollow fiber (PAN-ACHF) was immersed in a known volume of aqueous solution at 37°C for 24 h. The amount of creatinine and  $\text{VB}_{12}$  adsorbed was determined by the concentration difference before and after immersion in the solution. The creatinine and  $\text{VB}_{12}$  concentrations of the solution were determined with a UV-vis spectrophotometer (Shanghai Techcomp Corp. 7500) at the wavelength of 510 nm and 361 nm, respectively. Absorbency of creatinine and  $\text{VB}_{12}$  in the aqueous solutions reflects the difference of solution concentration. Then the adsorption ratio was calculated as follows:

Adsorption ratio (wt %)

$$= \frac{\text{Absorbency before adsorption} - \text{Absorbency after adsorption}}{\text{Absorbency before adsorption}} \times 100\%$$

Samples of PAN-ACHF were characterized by measuring specific BET surface area, surface area of mesopores, and pore size distribution using an auto-adsorption apparatus (Micromeritics Tristar 3000). The surface area was calculated using the multipoint BET method. Pore volume and pore size distribution were determined from the nitrogen adsorption isotherms using the Barrett, Joyner, and Halenda (BJH) method.<sup>15</sup>

## RESULTS AND DISCUSSION

### Surface area and adsorption properties of PAN-ACHF

By activating in  $\text{CO}_2$  at high temperature, micropores suitable for adsorption purpose would appear on the surface and the internal of the carbon fiber.<sup>4</sup> With the increasing of the temperature, the diffusion of  $\text{CO}_2$  into the defects of the molecular structure occurs, vigorous reaction caused the tunneling of the skin layer and the pores, and larger pores including mesopores were thus formed. So increasing activation temperature remarkably increases the number of micropores and mesopores.

When the carbon fibers were heated in  $\text{CO}_2$ , the carbon composition in the fiber reacted with the  $\text{CO}_2$  and evolved carbon monoxide.<sup>16</sup> This reaction led to a decrease in the weight of the resultant ACHF, as shown in Figure 2.

Figure 2 shows the variation in burn-off and shrinkage ratio of PAN-ACHF with activation temperature of ACHF. The weight loss and shrinkage ratio were determined from a change in weight and length before and after activation. We found that the weight loss of the fibers increases with activation temperature. The weight loss increases slowly before 800°C, then in-

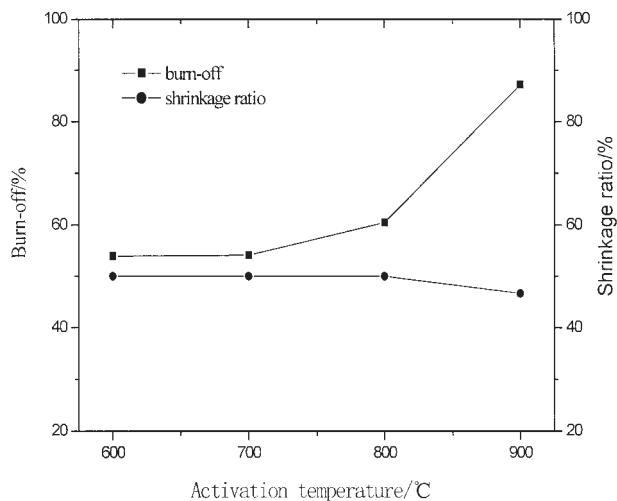


**Figure 2** Burn-off and shrinkage ratio of PAN-ACHF versus activation temperature.

creases sharply. The shrinkage ratio changes little over all activation temperature.

Figure 3 shows the variation in BET surface area of PAN-ACHF and surface area of mesopores in PAN-ACHF with activation temperature. Two reactions occurred simultaneously when the carbon fibers were heat-treated during activation. One was the formation of new carbon basal planes, which led to a denser structure, and another was the degradation by  $\text{CO}_2$ . When carbon fibers were heat-treated in  $\text{CO}_2$ , some structures of the fiber could be etched and removed. This reaction became more drastic and developed more pores with activation temperature increasing. As shown in Figure 3, BET surface area of PAN-ACHF and surface area of mesopores in PAN-ACHF increase slowly before 800°C, then increase sharply, and reach  $1422 \text{ m}^2 \text{ g}^{-1}$  and  $1234 \text{ m}^2 \text{ g}^{-1}$ , respectively. It is sug-

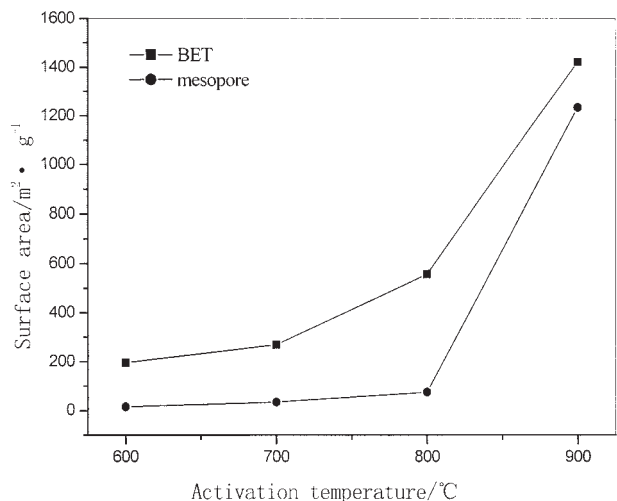


**Figure 3** Surface area of BET and mesopores versus activation temperature.

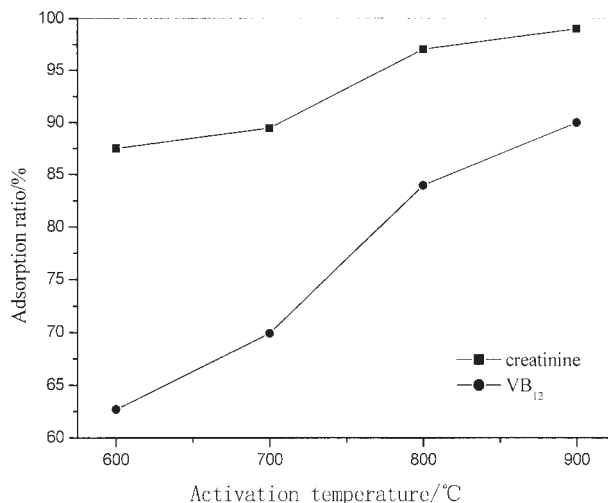


**Figure 4** Adsorption ratio of PAN-ACHF versus activation temperature.

gested that the pores in PAN-ACHF are mainly composed of mesopores.

Figure 4 shows the variation in adsorption ratio of PAN-ACHF with activation temperature of ACHF. The adsorption ratios to creatinine and  $\text{VB}_{12}$  gradually increase with activation temperature and reach 99 and 84% respectively, when activation temperature is 900°C. It is suggested that the number of micropores and mesopores in PAN-ACHF increases with activation temperature, and reaches the highest value when activation temperature is 900°C. This conclusion is in accordance with that obtained from the analysis of Figure 3.

#### Pore size distribution of PAN-ACHF

Figure 5 shows the pore size distribution of the PAN-ACHF made of fiber activated at 700°C, 800°C, and

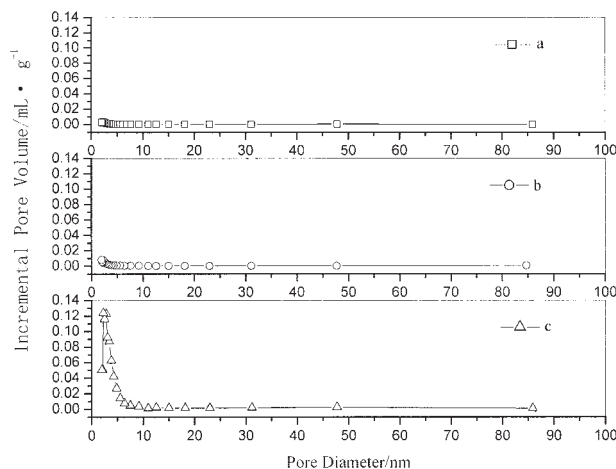


**Figure 5** Pore size distribution of PAN-ACHF (activation temperatures of a, b, and c are 700°C, 800°C, and 900°C respectively).

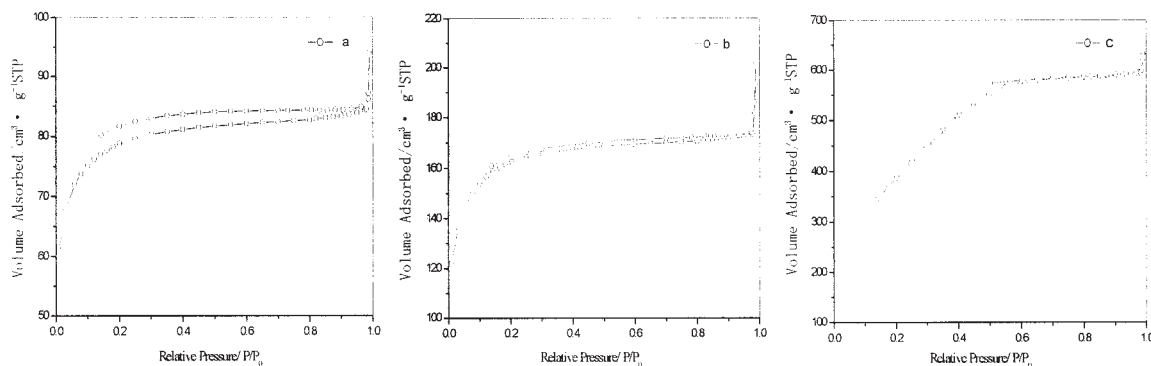


**Figure 6** Nitrogen adsorption isotherms of PAN-ACHF (activation temperatures of a, b, and c are 700°C, 800°C, and 900°C, respectively).

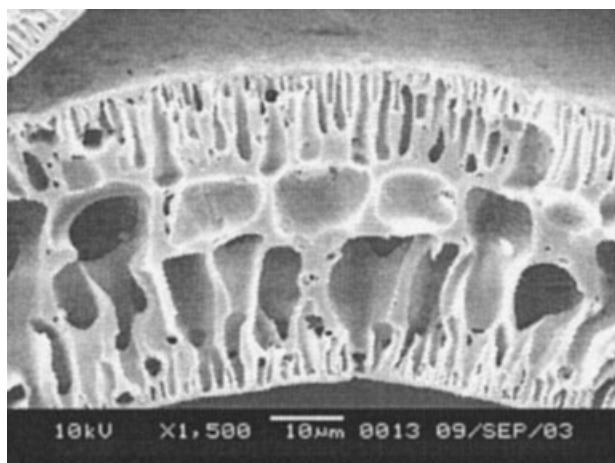
900°C for 40 min respectively. Because of the limits of apparatus, pore diameters of  $<2$  nm could not be tested. However, the distribution of mesopores (2–50 nm) and macropores ( $>50$  nm) can be observed by Figure 5. As shown in Figure 5, when the activation temperatures are 700°C and 800°C, the value of incremental pore volume with various pore diameter is low. As shown in Figure 3, the surface areas of mesopores in PAN-ACHF activated at 700°C and 800°C is much lower than those of PAN-ACHF activated at 900°C. It indicates that the pores in PAN-ACHF activated at 700°C and 800°C were mainly formed by micropores and just have a small quantity of mesopores. However, the surface area of mesopores in PAN-ACHF activated at 900°C reaches  $1234 \text{ m}^2 \text{ g}^{-1}$  (as shown in Fig. 3), and the dominant pore sizes of mesopores are from 2 to 5 nm (as shown in Fig. 5).

Figure 6 shows that nitrogen adsorption isotherms of PAN-ACHF made of fiber activated at 700°C, 800°C, and 900°C for 40 min, respectively. The nitrogen adsorption isotherms at 77 K presented in Figure 6 reflect the differences in porous texture among the PAN-ACHF that are studied in this work. Figure 6(a) and 6(b) present mixed Type II and IV isotherm in the IUPAC classification,<sup>17</sup> which shows adsorption isotherm rises sharply at low relative pressures and presents hysteresis at high relative pressures. It is suggested that in sample A and B, the micropore filling mainly occurred at low relative pressures, multimolecular layer adsorption occurred with relative pressure increasing, and the filling and emptying of the mesopores by capillary condensation occurred at high relative pressures. This phenomenon means that there are both of micropores and mesopores in samples A and B. Figure 6(c) presents Type II isotherm that shows quickly rising slope of the linear branch at higher relative pressures. It is suggested that in sample C, a mass of mesopores resulted in the large pore filling by capillary condensation.

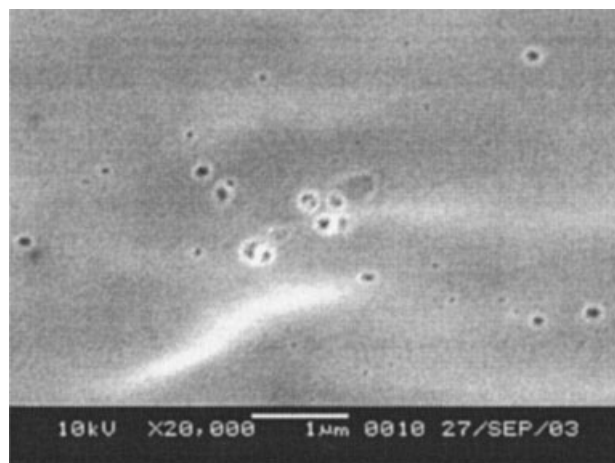
### Morphology of PAN-ACHF

Figure 7 shows the cross section of the PAN-ACHF made of the fiber activated at 700°C, 800°C, and 900°C for 40 min, respectively. The cross-sectional shapes of ACHF in Figure 7(a–c), difinger-like porous structure, are preserved after activation with  $\text{CO}_2$  and similar. It means that  $\text{CO}_2$  can not diffuse deeper to cause activation in the depth of the hollow fiber when activation temperature is not more than 900°C. When the carbon fibers were heated in  $\text{CO}_2$ , the carbon composition in the fiber reacted with the  $\text{CO}_2$  and evolved carbon monoxide. This reaction led to a decrease in the diameter of the resultant activated carbon fibers. As shown in Figure 7(a–c), compared with the thickness of fiber activated at 700°C and 800°C, that of fiber activated at 900°C obviously decreases. It means increasing activation temperature makes the reaction more drastic and the activation process reacts most drastically when activation temperature is 900°C.

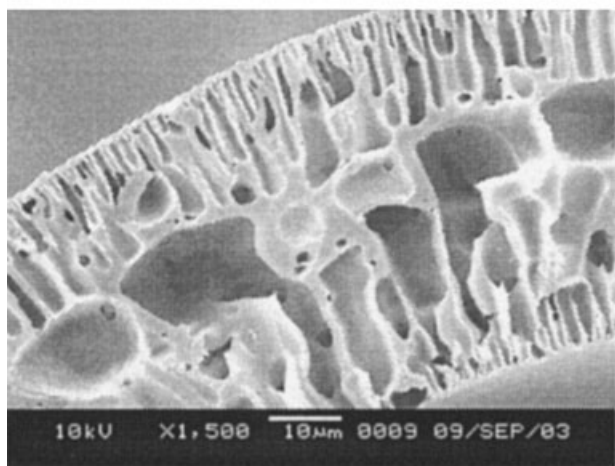
Figure 8 shows the external surface of the PAN-ACHF made of the fiber activated at 700°C, 800°C, and 900°C for 40 min, respectively. For an activation temperature of 700°C, there are a few pores, and white matters on the surface of ACHF are phosphate that is not reacted during reaction, as shown in Figure 8(a). It is because that carbon basal planes increasingly packed together and activation at lower temperature promoted the formation of ordered graphitoidal layer structure. This would hinder the diffusion of  $\text{CO}_2$  into the amorphous region to react with carbon.<sup>18</sup> After 800°C of activation, pores began to increase on the surface, as show in Figure 8(b). This suggests that the external surface and the thinner region of the skin of the hollow fibers have been activated. As shown in Figure 8(c), after 900°C of activation, the surface became composed of pores of uniform size. This indicates that the skin of the fibers was burned off, the molecules in the amorphous area were broken, and the closed pores were opened.



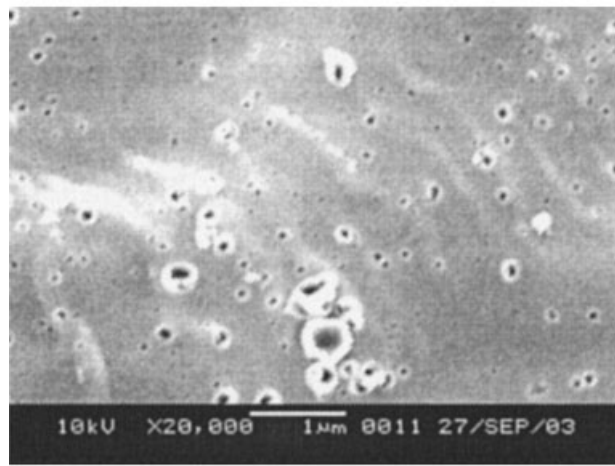
(a)



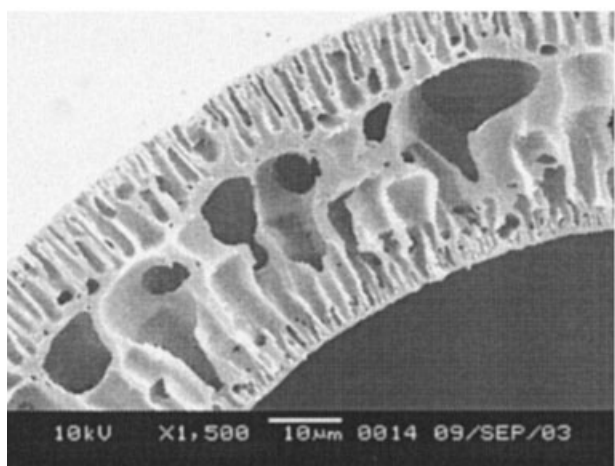
(a)



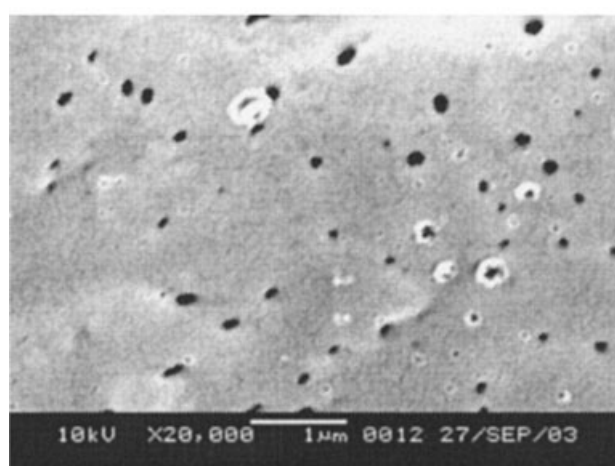
(b)



(b)



(c)



(c)

**Figure 7** SEM micrographs of the cross-sections of PAN-ACHF ( $\times 1500$ ) (activation temperatures of a, b, and c are  $700^{\circ}\text{C}$ ,  $800^{\circ}\text{C}$ , and  $900^{\circ}\text{C}$ , respectively).

**Figure 8** SEM micrographs of the external surface of PAN-ACHF ( $\times 20,000$ ) (activation temperatures of a, b, and c are  $700^{\circ}\text{C}$ ,  $800^{\circ}\text{C}$ ,  $900^{\circ}\text{C}$  respectively).

## CONCLUSIONS

The BET surface area of PAN-ACHF and surface area of mesopores gradually increases before 800°C of activation temperature, then remarkably increase when fibers are activated at 900°C for 40 min, and reach the maximum values, 1422 m<sup>2</sup> g<sup>-1</sup> and 1234 m<sup>2</sup> g<sup>-1</sup>, respectively. The different adsorption ratios to two adsorbates including creatinine and VB<sub>12</sub> also reach the maximum values, 99 and 84%. After the activation process, the cross-sectional shape of ACHF, difinger-like porous structure, is preserved. In PAN-ACHF which went through the activation at 700°C and 800°C, the micropore filling mainly occurred at low relative pressures, multimolecular layer adsorption occurred with increasing relative pressure, and the filling and emptying of the mesopores by capillary condensation occurred at high relative pressures. But in PAN-ACHF which went through the activation at 900°C, a mass of mesopores resulted in the large pore filling by capillary condensation. The pores in PAN-ACHF made of fibers activated at 900°C mainly consist of mesopores and the dominant pore sizes of mesopores in PAN-ACHF range from 2 nm to 5 nm.

## References

1. Mattson, J. S.; Mark, H. B. *Activated Carbon*; Marcel Dekker: New York, 1971.
2. McEnaney, B. *Carbon* 1988, 26, 267.
3. Wigmans, T. *Carbon* 1989, 27, 13.
4. Bansal, R. C.; Donnet, J. B.; Stoeckli, F. *Activate Carbon*; Marcel Dekker: New York, 1988.
5. Jaroniec, M.; Gilpin, R. K. *Langmuir* 1991, 7, 2719.
6. Jaroniec, M.; Gilpin, R. K. *Carbon* 1993, 31, 325.
7. Yang, M.-C.; Yu, D.-G. *J Appl Polym Sci* 1998, 58, 185.
8. Yang, M.-C.; Yu, D.-G. *Text Res J* 1996, 66, 115.
9. Yang, M.-C.; Yu, D.-G. *J Appl Polym Sci* 1996, 69, 1725.
10. Yang, M.-C.; Yu, D.-G. *J Appl Polym Sci* 1996, 62, 2287.
11. Linkov, V. M.; Sanderson, R. D.; Jacobs, E. P. *J Mat Sci* 1994, 95, 93.
12. Linkov, V. M.; Sanderson, R. D.; Jacobs, E. P. *Polym Int* 1994, 35, 239.
13. Linkov, V. M.; Sanderson, R. D.; Jacobs, E. P. *J Mat Sci Lett* 1994, 13, 600.
14. Schindler, E; Maier, F. U.S. Pat. 4,919,860, (1990).
15. Rist, L. P.; Harrison, D. P. *Fuel* 1985, 64, 291.
16. Grabke, H. *J Carbon* 1972, 10, 587.
17. Rouquerol, F.; Rouquerol, J.; Sing, K. *Adsorption by Powders and Porous Solids*; Academic Press: San Diego, 1999; p 18.
18. Yang, M.-C.; Yu, D.-G. *J Appl Polym Sci* 1998, 68, 1331.